Experimental Study on MHD Effect of Liquid Metal Sheath Jet for the Liquid Metal Divertor REVOLVER-D

Takuya GOTO[1,2], Takeru OHGO[2] and Junichi MIYAZAWA[1,2]

[1]*National Institute for Fusion Science, Toki, Gifu 509-5292 Japan*

[2]*The Graduate University for Advanced Studies, Toki, Gifu 509-5292 Japan*

(Received 28 January 2019 / Accepted 9 April 2019)

MHD effect of a liquid metal sheath jet, which is the jet stabilized by an inserted chain, has been experimentally investigated to examine its applicability to the divertor target of a fusion reactor. The deflection of the liquid metal jet together with the chain was observed when the electric current was applied to the jet under the presence of the magnetic field perpendicular to the jet flow direction. This means that the stabilization of the liquid meal jet by the chain is maintained when the jet is deformed by the magnetohydrodynamics (MHD) effect. However, the magnitude of the jet deflection agrees with the calculation result of the deflection of jet by the Lorentz force when the jet is regarded as a conductor. This indicates that mitigation of the Lorentz force and further investigation of the behavior of the liquid metal sheath jet under the exposure of divertor plasma is necessary to realize the divertor target using the liquid metal sheath jet.

© *2019 The Japan Society of Plasma Science and Nuclear Fusion Research*

Keywords: liquid metal divertor, free-falling jet, internal flow resistance, U-alloy78, MHD effect

DOI: 10.1585/pfr.14.1405092

1. Introduction

Conceptual design study of helical fusion reactor FFHR-c1 [1] has been conducted based upon the knowledge of the past design study of FFHR series and the achievements in the experiment of the Large Helical Device (LHD). FFHR-c1 aims at an early realization of a steady state operation with self-sufficiency of electricity and tritium fuel. Thus fusion output of FFHR-c1 is relatively small (~370 MW) compared with other typical power plant design. However, divertor heat load profile of LHD-type helical devices shows strong inhomogeneity. Consequently, the maximum local heat load on the divertor target can exceed 100 MW/m^2. To reduce the heat load, radiation cooling of SOL plasma and divertor detachment are generally taken into account. However, steady-state sustainment of these methods without the degradation of core plasma confinement property is not easily achieved. There are several other issues. These include continuous pumping, maintenance of 3D complicated structure and reduction of radioactive wastes.

To overcome these issues, a new concept of the liquid metal limiter/divertor, REVOLVER-D (Reactor-oriented Effective VOLumetric VERtical Divertor), has been proposed [2]. In this concept, multiple free-falling jets of liquid tin are used as a target. The jets are placed at the inboard side of 10 sections where plasma has a horizontally-elongated cross-sectional shape. The jets are inserted into the ergodized layer of magnetic lines of force that surrounds the core plasma. Approximately 90% of the plasma that heads to the divertor field lines is estimated to be removed by the jets. Several concepts of liquid metal divertor have already been proposed, such as capillary pore system [3], thermoelectric magnetohydrodynamics (TEMHD) flow [4], and others. REVOLVER-D has several advantages compared with these concepts. For example, it has a simple structure which consists of only ducts and pool. Thus, no complicated structure or mechanism is needed. The construction and maintenance work is also drastically simplified. High neutral gas pressure is expected because REVOLVER-D works as a local limiter. The neutralized gas can be easily pumped out through the gaps between the jets. Thus, high evacuation efficiency can be achieved. Because the temperature increase of the liquid tin can be controlled by adjusting the flow rate and the placement of the jets, power generation using the divertor heat is possible. The working fluid, tin, has several beneficial features: low evaporation pressure, high chemical stability, no toxicity, low radioactivity, and low cost.

On the other hand, there are several issues that must be examined in order to realize this concept. For example, these include heat removal, effect of tin vapor on the core plasma performance, compatibility with a structural material and tritium inventory. Among these issues, formation of a stable and continuous flow is essential. To avoid the transformation of the jets into droplets due to surface tension instability, the "sheath-jet" concept, that is, insertion of an internal flow resistance (IFR) (e.g., wires, tapes, and chains) to stabilize the jet, has been considered and its effectiveness has been confirmed by the experiment using water [5]. However, the stabilization effect

author's e-mail: goto.takuya@nifs.ac.jp

© 2019 The Japan Society of Plasma Science and Nuclear Fusion Research

must be examined using a liquid metal jet. In a fusion reactor, there exists a strong magnetic field and electric current can be passed through the jet due to the spatial variance of the electric potential of the plasma. Several experimental and theoretical studies have been performed for the effect of non-uniform magnetic field on a liquid metal jet [6–8]. However, no work has been performed for the liquid metal sheath jet and the behavior of the liquid metal sheath jet including the influence of MHD effect must be examined. Therefore, experiments using a small liquid metal circulation device have been conducted. The experimental setup and the experimental method are described in Sec. 2. The result and discussion are given in Sec. 3.

2. Experimental Setup

In order to generate a continuous liquid metal jet, a small liquid metal circulation device has been built. The photograph of the device is shown in Fig. 1. In this experiment, a low melting point alloy, U-alloy78 ($Bi_{57}In_{17}Sn_{26}$ with the melting point of 78°C), was used as a simulant of tin to reduce the issues in the thermal design and the material compatibility with the flow channel. The comparison of the material property of U-alloy78 and tin is summarized in Table 1. The flow channel is made of stainless steel (SUS403) and all sections of the loop can be heated up to 150°C. U-alloy78 is transported to the nozzle by a sealless magnet drive pump (SANWA MMH11). A continuous free-falling jet of U-alloy78 with a height of ~1 m and a maximum flow rate of ~9 L/min can be generated between the nozzle and the receiver. The diameter of the jet can be changed by attaching caps with a hole to the tip of the nozzle. The volumetric flow rate is measured by an electromagnetic flowmeter that is set at the vertical pipe section of the loop which lies downstream of the magnet drive pump. The jet section of the loop is installed in a glove box (W 1.2 m × D 1.0 m × H 1.5 m) and experiments are conducted under Argon atmosphere to avoid oxidation of U-alloy78.

In the case of the experiment for the examination of the MHD effect, two parallel permanent magnets with a rectangular shape (H 20 cm × W 10 cm) with a gap of 10 cm can be set under the nozzle (the vertical distance between the nozzle tip and the top edge of the magnet is 6 cm) and the magnetic field perpendicular to the jet flow direction can be generated. The magnetic field strength at the center of the magnet is ~0.23 T. Electric current can be directly applied to the jet through an aluminum mesh placed under the nozzle. The schematic of the setup for the MHD experiment is shown in Fig. 2. The magnetic field distribution along the jet direction measured by a Gauss meter is shown in Fig. 3.

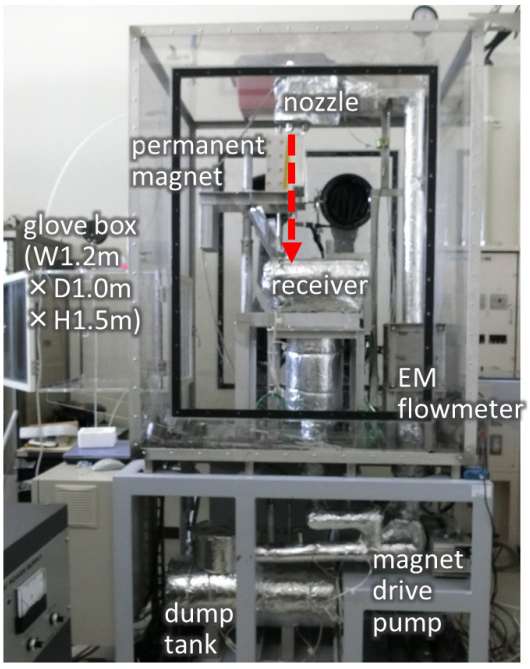

Fig. 1 Photograph of the experimental device.

3. Experimental Results

Prior to the MHD experiment, stabilization effect of liquid metal jet by the "sheath-jet" concept was examined. Figure 4 shows the photographs of the U-alloy78 jet at two different flow rates taken by a high-speed camera with an

Table 1 Material property of tin and U-alloy78.

Property	tin	U-alloy78
melting point [°C]	232	78
mass density [kg/m^3]	6990 (at 232°C)	8530 (at 100°C)
viscosity [10^{-6}m^2/s]	0.17	0.24
heat capacity [J/kg/K]	228 (25°C)	170 (25°C)
thermal conductivity [W/m/K]	66.8 (27°C)	9.6 (25°C)
electrical conductivity [10^6S/m]	7.9 (20°C)	1.3 (24°C)

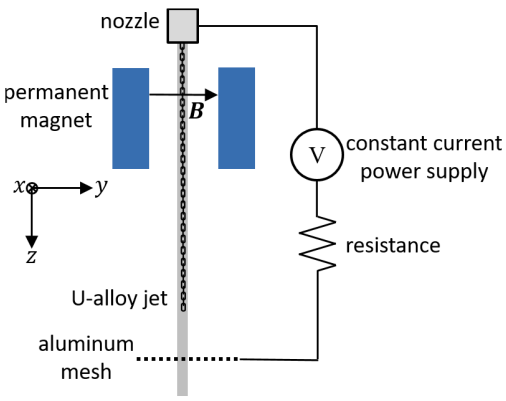

Fig. 2 Schematics of the experimental setup. The origin of the Cartesian coordinate is set just below the nozzle.

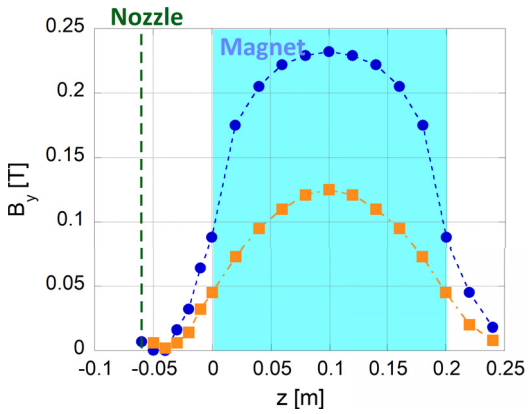

Fig. 3 Profile of magnetic field strength along the jet direction at the center of the magnet ($x = y = 0$ m, circle symbols) and the edge of the magnet ($x = 0.05$ m, $y = 0$ m, square symbols).

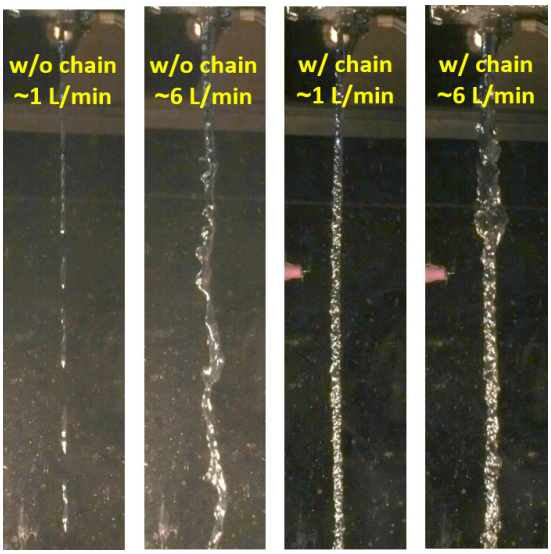

Fig. 4 Photographs of the U-alloy jet with and without the IFR (chain) at two different flow rates (1 L/min and 6 L/min) taken by the exposure time of 1/2000 sec.

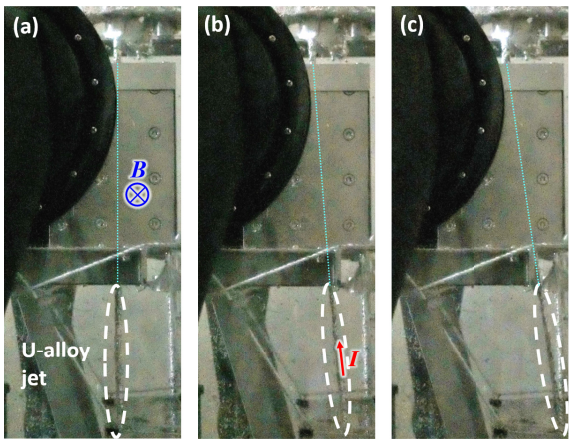

Fig. 5 Photographs of the liquid metal jet with an aluminum chain at the applied electric current of (a) 0 A, (b) 3 A and (c) 6 A. Broken lines indicate expected trajectory of the jet.

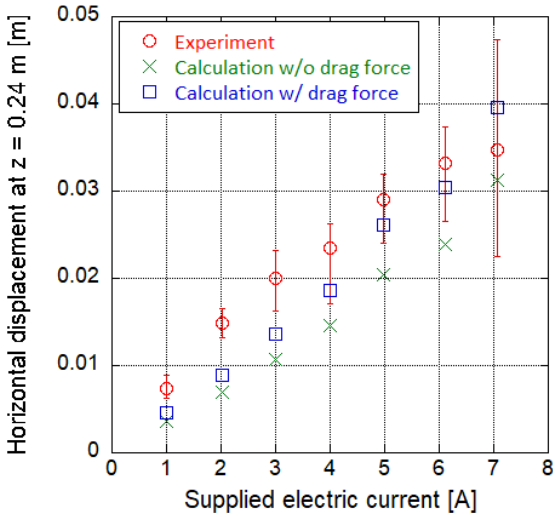

Fig. 6 Horizontal displacement of the jet at the bottom edge of the magnet support structure (300 mm below the nozzle). Open circle symbols are the experimental result. Cross symbols are the calculation result using Eqs. (7) - (8). Open square symbols are the calculation result with a consideration of the drag force.

exposure time of 1/2000 sec. A stainless steel chain with the width of 5 mm was used as the IFR. The jet without the IFR finally becomes droplets at a low flow rate (~1 L/min). At a high flow rate (~6 L/min), the jet becomes continuous but is strongly deformed. On the other hand, the jet with the IFR is stable and continuous irrespective of the flow rate. Consequently, the stabilization effect of the IFR has been confirmed in the case of liquid metal jets.

Figure 5 shows the photographs of the U-alloy78 sheath jet with the magnetic field at different electric currents. In this experiment, a nozzle with the diameter of 10 mm and an aluminum chain with the width of 5 mm were used. The reason why an aluminum chain was used in this experiment instead of a stainless steel chain is that aluminum is non-magnetic material and is not affected by the magnetic field. (Experiments with a larger diameter of the jet were planned, but a stable full filled flow with larger nozzles could not be achieved due to the instability of the flow rate at a high flow rate.) As shown in Fig. 5, the jet was deflected together with the chain. This indicates that the stabilization of the jet is maintained if the jet is deformed by the MHD effect. The deflection becomes larger as the increase of the electric current. The horizontal displacement measured at the bottom edge of the magnet support structure (24 cm below the nozzle) is plotted in Fig. 6 with open circle symbols. The displacement seems to be proportional to the applied electric current.

To evaluate the relation between the deflection and the electric current in a quantitative way, a calculation was

conducted using the equation of the motion

$$\rho \frac{\mathrm{d}\boldsymbol{u}}{\mathrm{d}t} = \rho \boldsymbol{g} + \boldsymbol{j} \times \boldsymbol{B}, \tag{1}$$

where ρ, $\boldsymbol{u}$, $\boldsymbol{g}$ and $\boldsymbol{B}$ are the mass density of the liquid, velocity of the liquid, acceleration of gravity and magnetic field, respectively. The current density $\boldsymbol{j}$ is the sum of the externally applied current and the current that caused by the change in the electric field and magnetic field

$$\boldsymbol{j} = \boldsymbol{j}_{\mathrm{ext}} + \boldsymbol{j}_{\mathrm{in}}. \tag{2}$$

It is assumed that the applied electric current flows along the jet with a homogeneous current density profile over the jet cross-section and the jet maintains its circular cross-sectional shape. Then, the current density of the supplied electric current is given as

$$j_{\mathrm{ext}} \equiv |\boldsymbol{j}_{\mathrm{ext}}| = I_{\mathrm{ext}} \Big/ \left(\frac{\pi d^2}{4} \right), \tag{3}$$

where I_{ext} and d are the applied electric current value and the diameter of the jet cross-section. Because the flow rate is constant at any position of the jet, the jet diameter d can be calculated using the vertical velocity of the jet u_z:

$$d(z) = d_0 \left(\frac{u_{z0}}{u_z(z)} \right)^2, \tag{4}$$

where d_0 and u_{z0} are the nozzle diameter and the initial velocity of the jet (calculated from the flow rate $Q = \pi d_0^2 u_{z0}/4$). The current density of the eddy current is calculated by the following formulae:

$$\boldsymbol{j}_{\mathrm{in}} = \sigma \left(\boldsymbol{E} + \boldsymbol{u} \times \boldsymbol{B} \right), \tag{5}$$

$$\nabla \times \boldsymbol{E} = -\frac{\partial \boldsymbol{B}}{\partial t}, \tag{6}$$

where σ is the electric conductivity of U-alloy78. For simplicity, only the magnetic field generated by the permanent magnet is considered: $\boldsymbol{B} = B_{\mathrm{y}} \boldsymbol{e}_y$. Then, Eq. (1) is reduced to the following two equations:

$$\rho \frac{\mathrm{d}u_x}{\mathrm{d}t} = -j_z B_y = -j_{\mathrm{ext}} B_y - \sigma (E_z B_y - u_x B_y^2), \tag{7}$$

$$\rho \frac{\mathrm{d}u_z}{\mathrm{d}t} = \rho g + j_x B_y = \rho g + \sigma (E_x B_y - u_z B_y^2). \tag{8}$$

Using the above equations and the magnetic field profile given in Fig. 3, the horizontal displacement of the jet at the bottom edge of the magnet supporting structure (z = 0.24 m) is estimated. The result is plotted by cross symbols in Fig. 6. The calculated values are smaller than those of the experimental observation. One possible reason for this discrepancy is the deceleration of the jet due to the drag force caused by the friction with the IFR. In the experiment using water, the sheath jet has the terminal velocity that is a function of the volumetric flow rate Q and the circumference of the IFR: $v_{\mathrm{t}} \propto C^{-0.26} Q^{0.36}$ [5]. If this scaling can be applied to the liquid metal sheath jet, the terminal velocity is expected to be ∼1.7 m/s, which is smaller than the calculated jet velocity u_z at z = 0.24 m. Thus, the calculation with a consideration of the drag force was also conducted. It is assumed that the drag force is proportional to the square of the velocity ($F_{\mathrm{drag}} \propto c_D \rho u^2$) from the analogy of the friction loss of pipe flow. The drag coefficient c_D is determined to reproduce the terminal velocity of 1.7 m/s, that is, $c_D \propto g/1.7^2$. The results are also plotted in Fig. 6. Though there still remains some discrepancy at low electric current region, calculation result is consistent with the experimental observation considering the error in the measurement of the flow velocity and the assumptions in the calculation. Consequently, it can be concluded that the behavior of a liquid metal sheath jet can be explained by the Lorentz force. In other words, a liquid metal sheath jet acts just as a normal liquid metal jet or a single flexible conductor.

The experiment shows that the liquid metal sheath jet can be deflected with the order of 1 cm with a magnetic field with the order of 0.1 T and an electric current with the order of 1 A. In a fusion reactor environment, the magnetic field strength at the divertor region reaches several Tesla. For example, the magnetic field strength will be 5 T in the helical fusion reactor FFHR-c1. Though the estimation of the electric current from the divertor plasma is quite difficult, it is considered to be of the same order as the ion saturation current. The ion saturation current per a unit area is expected to be the order of 100 kA/m^2 in the reactor condition [2]. Thus, it can be the order of 100 A with the assumed jet diameter in the reactor of ∼0.03 m. Then the Lorentz force in a fusion reactor can reach several thousand times larger than that in this experiment and unacceptable deflection will occur. This indicates that significant reduction of the electric current from divertor plasma or disconnection of the current path is necessary to apply the liquid metal sheath jets as the divertor target. The former can be realized by the detachment by a gas puffing. As mentioned above, steady-state sustainment of the detachment is not easy. However, short-time failure of the detachment may be acceptable because the liquid metal flow is renewable. In the actual condition in a fusion reactor, the electric current is considered to not be a constant. Thus, the absolute value and the radial profile of the electric current can differ from the estimation from this experiment due to the skin effect. Experiments with plasma exposure are required to examine these effects. The latter method, disconnection of the current path, can be realized by the formation of dense droplets. However, control of the size and the interval of droplets without complicated mechanism is difficult. Regarding this, the use of solid tin pebbles instead of the liquid tin jet can be a solution.

4. Summary

Flow characteristics of the liquid metal "sheath-jet" were investigated using a small liquid metal circulation device. It was found that the liquid metal jet is stabilized by

the internal flow resistance similar to the water jet, and the jet is deflected together with the internal flow resistance. The behavior of the jet can be explained by the Lorentz force which acts on the jet without the IFR. The experimental results indicate that the stabilization effect of the jet by the IFR can be maintained under the deformation of the jet. However, deflection in a fusion reactor environment is estimated to be an unacceptable level.

In conclusion, significant reduction of the electric current from plasma and/or the disconnection of the current path is necessary to apply the liquid metal sheath jet to the divertor target of a fusion reactor. Experiments under the plasma exposure are being considered to examine these countermeasures.

This work is supported by MEXT/JSPS KAKENHI Grant Number 16H06140, 16K14530 and the budget NIFS10UFFF038 of National Institute for Fusion Science. The authors also appreciate the members of the Fusion Engineering Research Project in NIFS for providing valuable comments and advice.

[1] J. Miyazawa *et al.*, Fusion Eng. Des. **136**, 1278 (2018).
[2] J. Miyazawa *et al*., Fusion Eng. Des. **125**, 227 (2017).
[3] S.V. Mirnov *et al.*, Plasma Phys. Control. Fusion **48**, 821 (2006).
[4] D.N. Ruzic *et al.*, Nucl. Fusion **51**, 102002 (2011).
[5] T. Ohgo *et al.*, Plasma Fusion Res. **13**, 1405003 (2018).
[6] S. Oshima *et al.*, JSME Int. J. **30**, 437 (1987).
[7] Z. Xu *et al.*, Fusion Sci. Technol. **46**, 577 (2004).
[8] W. Kang *et al.*, Fusion Eng. Des. **81**, 1019 (2006).